Fermilab-Pub-07/668-E

Search for squarks and gluinos in events with jets and missing transverse energy using 2.1 fb^{-1} of $p\bar{p}$ collision data at $\sqrt{s}$ =1.96 TeV

V.M. Abazov[36], B. Abbott[76], M. Abolins[66], B.S. Acharya[29], M. Adams[52], T. Adams[50], E. Aguilo[6], S.H. Ahn[31], M. Ahsan[60], G.D. Alexeev[36], G. Alkhazov[40], A. Alton[65,a], G. Alverson[64], G.A. Alves[2], M. Anastasoaie[35], L.S. Ancu[35], T. Andeen[54], S. Anderson[46], B. Andrieu[17], M.S. Anzelc[54], Y. Arnoud[14], M. Arov[61], M. Arthaud[18], A. Askew[50], B. Åsman[41], A.C.S. Assis Jesus[3], O. Atramentov[50], C. Autermann[21], C. Avila[8], C. Ay[24], F. Badaud[13], A. Baden[62], L. Bagby[53], B. Baldin[51], D.V. Bandurin[60], S. Banerjee[29], P. Banerjee[29], E. Barberis[64], A.-F. Barfuss[15], P. Bargassa[81], P. Baringer[59], J. Barreto[2], J.F. Bartlett[51], U. Bassler[18], D. Bauer[44], S. Beale[6], A. Bean[59], M. Begalli[3], M. Begel[72], C. Belanger-Champagne[41], L. Bellantoni[51], A. Bellavance[51], J.A. Benitez[66], S.B. Beri[27], G. Bernardi[17], R. Bernhard[23], I. Bertram[43], M. Besançon[18], R. Beuselinck[44], V.A. Bezzubov[39], P.C. Bhat[51], V. Bhatnagar[27], C. Biscarat[20], G. Blazey[53], F. Blekman[44], S. Blessing[50], D. Bloch[19], K. Bloom[68], A. Boehnlein[51], D. Boline[63], T.A. Bolton[60], G. Borissov[43], T. Bose[78], A. Brandt[79], R. Brock[66], G. Brooijmans[71], A. Bross[51], D. Brown[82], N.J. Buchanan[50], D. Buchholz[54], M. Buehler[82], V. Buescher[22], V. Bunichev[38], S. Burdin[43,b], S. Burke[46], T.H. Burnett[83], C.P. Buszello[44], J.M. Butler[63], P. Calfayan[25], S. Calvet[16], J. Cammin[72], W. Carvalho[3], B.C.K. Casey[51], N.M. Cason[56], H. Castilla-Valdez[33], S. Chakrabarti[18], D. Chakraborty[53], K.M. Chan[56], K. Chan[6], A. Chandra[49], F. Charles[19,‡], E. Cheu[46], F. Chevallier[14], D.K. Cho[63], S. Choi[32], B. Choudhary[28], L. Christofek[78], T. Christoudias[44,†], S. Cihangir[51], D. Claes[68], Y. Coadou[6], M. Cooke[81], W.E. Cooper[51], M. Corcoran[81], F. Couderc[18], M.-C. Cousinou[15], S. Crépé-Renaudin[14], D. Cutts[78], M. Ćwiok[30], H. da Motta[2], A. Das[46], G. Davies[44], K. De[79], S.J. de Jong[35], E. De La Cruz-Burelo[65], C. De Oliveira Martins[3], J.D. Degenhardt[65], F. Déliot[18], M. Demarteau[51], R. Demina[72], D. Denisov[51], S.P. Denisov[39], S. Desai[51], H.T. Diehl[51], M. Diesburg[51], A. Dominguez[68], H. Dong[73], L.V. Dudko[38], L. Duflot[16], S.R. Dugad[29], D. Duggan[50], A. Duperrin[15], J. Dyer[66], A. Dyshkant[53], M. Eads[68], D. Edmunds[66], J. Ellison[49], V.D. Elvira[51], Y. Enari[78], S. Eno[62], P. Ermolov[38], H. Evans[55], A. Evdokimov[74], V.N. Evdokimov[39], A.V. Ferapontov[60], T. Ferbel[72], F. Fiedler[24], F. Filthaut[35], W. Fisher[51], H.E. Fisk[51], M. Ford[45], M. Fortner[53], H. Fox[23], S. Fu[51], S. Fuess[51], T. Gadfort[71], C.F. Galea[35], E. Gallas[51], E. Galyaev[56], C. Garcia[72], A. Garcia-Bellido[83], V. Gavrilov[37], P. Gay[13], W. Geist[19], D. Gelé[19], C.E. Gerber[52], Y. Gershtein[50], D. Gillberg[6], G. Ginther[72], N. Gollub[41], B. Gómez[8], A. Goussiou[56], P.D. Grannis[73], H. Greenlee[51], Z.D. Greenwood[61], E.M. Gregores[4], G. Grenier[20], Ph. Gris[13], J.-F. Grivaz[16], A. Grohsjean[25], S. Grünendahl[51], M.W. Grünewald[30], J. Guo[73], F. Guo[73], P. Gutierrez[76], G. Gutierrez[51], A. Haas[71], N.J. Hadley[62], P. Haefner[25], S. Hagopian[50], J. Haley[69], I. Hall[66], R.E. Hall[48], L. Han[7], P. Hansson[41], K. Harder[45], A. Harel[72], R. Harrington[64], J.M. Hauptman[58], R. Hauser[66], J. Hays[44], T. Hebbeker[21], D. Hedin[53], J.G. Hegeman[34], J.M. Heinmiller[52], A.P. Heinson[49], U. Heintz[63], C. Hensel[59], K. Herner[73], G. Hesketh[64], M.D. Hildreth[56], R. Hirosky[82], J.D. Hobbs[73], B. Hoeneisen[12], H. Hoeth[26], M. Hohlfeld[22], S.J. Hong[31], S. Hossain[76], P. Houben[34], Y. Hu[73], Z. Hubacek[10], V. Hynek[9], I. Iashvili[70], R. Illingworth[51], A.S. Ito[51], S. Jabeen[63], M. Jaffré[16], S. Jain[76], K. Jakobs[23], C. Jarvis[62], R. Jesik[44], K. Johns[46], C. Johnson[71], M. Johnson[51], A. Jonckheere[51], P. Jonsson[44], A. Juste[51], E. Kajfasz[15], A.M. Kalinin[36], J.R. Kalk[66], J.M. Kalk[61], S. Kappler[21], D. Karmanov[38], P.A. Kasper[51], I. Katsanos[71], D. Kau[50], R. Kaur[27], V. Kaushik[79], R. Kehoe[80], S. Kermiche[15], N. Khalatyan[51], A. Khanov[77], A. Kharchilava[70], Y.M. Kharzheev[36], D. Khatidze[71], T.J. Kim[31], M.H. Kirby[54], M. Kirsch[21], B. Klima[51], J.M. Kohli[27], J.-P. Konrath[23], V.M. Korablev[39], A.V. Kozelov[39], D. Krop[55], T. Kuhl[24], A. Kumar[70], S. Kunori[62], A. Kupco[11], T. Kurča[20], J. Kvita[9,†], F. Lacroix[13], D. Lam[56], S. Lammers[71], G. Landsberg[78], P. Lebrun[20], W.M. Lee[51], A. Leflat[38], F. Lehner[42], J. Lellouch[17], J. Leveque[46], J. Li[79], Q.Z. Li[51], L. Li[49], S.M. Lietti[5], J.G.R. Lima[53], D. Lincoln[51], J. Linnemann[66], V.V. Lipaev[39], R. Lipton[51], Y. Liu[7,†], Z. Liu[6], A. Lobodenko[40], M. Lokajicek[11], P. Love[43], H.J. Lubatti[83], R. Luna[3], A.L. Lyon[51], A.K.A. Maciel[2], D. Mackin[81], R.J. Madaras[47], P. Mättig[26], C. Magass[21], A. Magerkurth[65], P.K. Mal[56], H.B. Malbouisson[3], S. Malik[68], V.L. Malyshev[36], H.S. Mao[51], Y. Maravin[60], B. Martin[14], R. McCarthy[73], A. Melnitchouk[67], L. Mendoza[8], P.G. Mercadante[5], M. Merkin[38], K.W. Merritt[51], J. Meyer[22,d], A. Meyer[21], T. Millet[20], J. Mitrevski[71], J. Molina[3], R.K. Mommsen[45], N.K. Mondal[29], R.W. Moore[6], T. Moulik[59], G.S. Muanza[20], M. Mulders[51], M. Mulhearn[71], O. Mundal[22], L. Mundim[3], E. Nagy[15], M. Naimuddin[51], M. Narain[78], N.A. Naumann[35], H.A. Neal[65], J.P. Negret[8], P. Neustroev[40], H. Nilsen[23], H. Nogima[3], S.F. Novaes[5], T. Nunnemann[25], V. O'Dell[51], D.C. O'Neil[6], G. Obrant[40], C. Ochando[16], D. Onoprienko[60], N. Oshima[51], J. Osta[56], R. Otec[10], G.J. Otero y Garzón[51], M. Owen[45],

P. Padley[81], M. Pangilinan[78], N. Parashar[57], S.-J. Park[72], S.K. Park[31], J. Parsons[71], R. Partridge[78], N. Parua[55], A. Patwa[74], G. Pawloski[81], B. Penning[23], M. Perfilov[38], K. Peters[45], Y. Peters[26], P. Pétroff[16], M. Petteni[44], R. Piegaia[1], J. Piper[66], M.-A. Pleier[22], P.L.M. Podesta-Lerma[33,c], V.M. Podstavkov[51], Y. Pogorelov[56], M.-E. Pol[2], P. Polozov[37], B.G. Pope[66], A.V. Popov[39], C. Potter[6], W.L. Prado da Silva[3], H.B. Prosper[50], S. Protopopescu[74], J. Qian[65], A. Quadt[22,d], B. Quinn[67], A. Rakitine[43], M.S. Rangel[2], K. Ranjan[28], P.N. Ratoff[43], P. Renkel[80], S. Reucroft[64], P. Rich[45], J. Rieger[55], M. Rijssenbeek[73], I. Ripp-Baudot[19], F. Rizatdinova[77], S. Robinson[44], R.F. Rodrigues[3], M. Rominsky[76], C. Royon[18], P. Rubinov[51], R. Ruchti[56], G. Safronov[37], G. Sajot[14], A. Sánchez-Hernández[33], M.P. Sanders[17], A. Santoro[3], G. Savage[51], L. Sawyer[61], T. Scanlon[44], D. Schaile[25], R.D. Schamberger[73], Y. Scheglov[40], H. Schellman[54], T. Schliephake[26], C. Schwanenberger[45], A. Schwartzman[69], R. Schwienhorst[66], J. Sekaric[50], H. Severini[76], E. Shabalina[52], M. Shamim[60], V. Shary[18], A.A. Shchukin[39], R.K. Shivpuri[28], V. Siccardi[19], V. Simak[10], V. Sirotenko[51], P. Skubic[76], P. Slattery[72], D. Smirnov[56], J. Snow[75], G.R. Snow[68], S. Snyder[74], S. Söldner-Rembold[45], L. Sonnenschein[17], A. Sopczak[43], M. Sosebee[79], K. Soustruznik[9], B. Spurlock[79], J. Stark[14], J. Steele[61], V. Stolin[37], D.A. Stoyanova[39], J. Strandberg[65], S. Strandberg[41], M.A. Strang[70], M. Strauss[76], E. Strauss[73], R. Ströhmer[25], D. Strom[54], L. Stutte[51], S. Sumowidagdo[50], P. Svoisky[56], A. Sznajder[3], M. Talby[15], P. Tamburello[46], A. Tanasijczuk[1], W. Taylor[6], J. Temple[46], B. Tiller[25], F. Tissandier[13], M. Titov[18], V.V. Tokmenin[36], T. Toole[62], I. Torchiani[23], T. Trefzger[24], D. Tsybychev[73], B. Tuchming[18], C. Tully[69], P.M. Tuts[71], R. Unalan[66], S. Uvarov[40], L. Uvarov[40], S. Uzunyan[53], B. Vachon[6], P.J. van den Berg[34], R. Van Kooten[55], W.M. van Leeuwen[34], N. Varelas[52], E.W. Varnes[46], I.A. Vasilyev[39], M. Vaupel[26], P. Verdier[20], L.S. Vertogradov[36], M. Verzocchi[51], F. Villeneuve-Seguier[44], P. Vint[44], P. Vokac[10], E. Von Toerne[60], M. Voutilainen[68,e], R. Wagner[69], H.D. Wahl[50], L. Wang[62], M.H.L.S Wang[51], J. Warchol[56], G. Watts[83], M. Wayne[56], M. Weber[51], G. Weber[24], L. Welty-Rieger[55], A. Wenger[42], N. Wermes[22], M. Wetstein[62], A. White[79], D. Wicke[26], G.W. Wilson[59], S.J. Wimpenny[49], M. Wobisch[61], D.R. Wood[64], T.R. Wyatt[45], Y. Xie[78], S. Yacoob[54], R. Yamada[51], M. Yan[62], T. Yasuda[51], Y.A. Yatsunenko[36], K. Yip[74], H.D. Yoo[78], S.W. Youn[54], J. Yu[79], A. Zatserklyaniy[53], C. Zeitnitz[26], T. Zhao[83], B. Zhou[65], J. Zhu[73], M. Zielinski[72], D. Zieminska[55], A. Zieminski[55,‡], L. Zivkovic[71], V. Zutshi[53], and E.G. Zverev[38]

(The DØ Collaboration)

[1] *Universidad de Buenos Aires, Buenos Aires, Argentina*
[2] *LAFEX, Centro Brasileiro de Pesquisas Físicas, Rio de Janeiro, Brazil*
[3] *Universidade do Estado do Rio de Janeiro, Rio de Janeiro, Brazil*
[4] *Universidade Federal do ABC, Santo André, Brazil*
[5] *Instituto de Física Teórica, Universidade Estadual Paulista, São Paulo, Brazil*
[6] *University of Alberta, Edmonton, Alberta, Canada, Simon Fraser University, Burnaby, British Columbia, Canada, York University, Toronto, Ontario, Canada, and McGill University, Montreal, Quebec, Canada*
[7] *University of Science and Technology of China, Hefei, People's Republic of China*
[8] *Universidad de los Andes, Bogotá, Colombia*
[9] *Center for Particle Physics, Charles University, Prague, Czech Republic*
[10] *Czech Technical University, Prague, Czech Republic*
[11] *Center for Particle Physics, Institute of Physics, Academy of Sciences of the Czech Republic, Prague, Czech Republic*
[12] *Universidad San Francisco de Quito, Quito, Ecuador*
[13] *LPC, Univ Blaise Pascal, CNRS/IN2P3, Clermont, France*
[14] *LPSC, Université Joseph Fourier Grenoble 1, CNRS/IN2P3, Institut National Polytechnique de Grenoble, France*
[15] *CPPM, IN2P3/CNRS, Université de la Méditerranée, Marseille, France*
[16] *LAL, Univ Paris-Sud, IN2P3/CNRS, Orsay, France*
[17] *LPNHE, IN2P3/CNRS, Universités Paris VI and VII, Paris, France*
[18] *DAPNIA/Service de Physique des Particules, CEA, Saclay, France*
[19] *IPHC, Université Louis Pasteur et Université de Haute Alsace, CNRS/IN2P3, Strasbourg, France*
[20] *IPNL, Université Lyon 1, CNRS/IN2P3, Villeurbanne, France and Université de Lyon, Lyon, France*
[21] *III. Physikalisches Institut A, RWTH Aachen, Aachen, Germany*
[22] *Physikalisches Institut, Universität Bonn, Bonn, Germany*
[23] *Physikalisches Institut, Universität Freiburg, Freiburg, Germany*
[24] *Institut für Physik, Universität Mainz, Mainz, Germany*
[25] *Ludwig-Maximilians-Universität München, München, Germany*

[26] *Fachbereich Physik, University of Wuppertal, Wuppertal, Germany*
[27] *Panjab University, Chandigarh, India*
[28] *Delhi University, Delhi, India*
[29] *Tata Institute of Fundamental Research, Mumbai, India*
[30] *University College Dublin, Dublin, Ireland*
[31] *Korea Detector Laboratory, Korea University, Seoul, Korea*
[32] *SungKyunKwan University, Suwon, Korea*
[33] *CINVESTAV, Mexico City, Mexico*
[34] *FOM-Institute NIKHEF and University of Amsterdam/NIKHEF, Amsterdam, The Netherlands*
[35] *Radboud University Nijmegen/NIKHEF, Nijmegen, The Netherlands*
[36] *Joint Institute for Nuclear Research, Dubna, Russia*
[37] *Institute for Theoretical and Experimental Physics, Moscow, Russia*
[38] *Moscow State University, Moscow, Russia*
[39] *Institute for High Energy Physics, Protvino, Russia*
[40] *Petersburg Nuclear Physics Institute, St. Petersburg, Russia*
[41] *Lund University, Lund, Sweden, Royal Institute of Technology and Stockholm University, Stockholm, Sweden, and Uppsala University, Uppsala, Sweden*
[42] *Physik Institut der Universität Zürich, Zürich, Switzerland*
[43] *Lancaster University, Lancaster, United Kingdom*
[44] *Imperial College, London, United Kingdom*
[45] *University of Manchester, Manchester, United Kingdom*
[46] *University of Arizona, Tucson, Arizona 85721, USA*
[47] *Lawrence Berkeley National Laboratory and University of California, Berkeley, California 94720, USA*
[48] *California State University, Fresno, California 93740, USA*
[49] *University of California, Riverside, California 92521, USA*
[50] *Florida State University, Tallahassee, Florida 32306, USA*
[51] *Fermi National Accelerator Laboratory, Batavia, Illinois 60510, USA*
[52] *University of Illinois at Chicago, Chicago, Illinois 60607, USA*
[53] *Northern Illinois University, DeKalb, Illinois 60115, USA*
[54] *Northwestern University, Evanston, Illinois 60208, USA*
[55] *Indiana University, Bloomington, Indiana 47405, USA*
[56] *University of Notre Dame, Notre Dame, Indiana 46556, USA*
[57] *Purdue University Calumet, Hammond, Indiana 46323, USA*
[58] *Iowa State University, Ames, Iowa 50011, USA*
[59] *University of Kansas, Lawrence, Kansas 66045, USA*
[60] *Kansas State University, Manhattan, Kansas 66506, USA*
[61] *Louisiana Tech University, Ruston, Louisiana 71272, USA*
[62] *University of Maryland, College Park, Maryland 20742, USA*
[63] *Boston University, Boston, Massachusetts 02215, USA*
[64] *Northeastern University, Boston, Massachusetts 02115, USA*
[65] *University of Michigan, Ann Arbor, Michigan 48109, USA*
[66] *Michigan State University, East Lansing, Michigan 48824, USA*
[67] *University of Mississippi, University, Mississippi 38677, USA*
[68] *University of Nebraska, Lincoln, Nebraska 68588, USA*
[69] *Princeton University, Princeton, New Jersey 08544, USA*
[70] *State University of New York, Buffalo, New York 14260, USA*
[71] *Columbia University, New York, New York 10027, USA*
[72] *University of Rochester, Rochester, New York 14627, USA*
[73] *State University of New York, Stony Brook, New York 11794, USA*
[74] *Brookhaven National Laboratory, Upton, New York 11973, USA*
[75] *Langston University, Langston, Oklahoma 73050, USA*
[76] *University of Oklahoma, Norman, Oklahoma 73019, USA*
[77] *Oklahoma State University, Stillwater, Oklahoma 74078, USA*
[78] *Brown University, Providence, Rhode Island 02912, USA*
[79] *University of Texas, Arlington, Texas 76019, USA*
[80] *Southern Methodist University, Dallas, Texas 75275, USA*
[81] *Rice University, Houston, Texas 77005, USA*
[82] *University of Virginia, Charlottesville, Virginia 22901, USA and*
[83] *University of Washington, Seattle, Washington 98195, USA*

(Dated: January 24, 2008)

A data sample corresponding to an integrated luminosity of $2.1\,\mathrm{fb}^{-1}$ collected by the D0 detector at the Fermilab Tevatron Collider was analyzed to search for squarks and gluinos produced in $p\bar{p}$ collisions at a center-of-mass energy of 1.96 TeV. No evidence for the production of such particles

was observed in topologies involving jets and missing transverse energy, and 95% C.L. lower limits of 379 GeV and 308 GeV were set on the squark and gluino masses, respectively, within the framework of minimal supergravity with $\tan\beta = 3$, $A_0 = 0$, and $\mu < 0$. The corresponding previous limits are improved by 54 GeV and 67 GeV.

PACS numbers: 14.80.Ly, 12.60.Jv, 13.85.Rm

In supersymmetric models [1], each of the standard model (SM) particles has a partner differing by a half-unit of spin. If R-parity [2] is conserved, supersymmetric particles are produced in pairs, and their decay leads to SM particles and to the lightest supersymmetric particle (LSP), which is stable. Cosmological arguments suggest that the LSP should be neutral and colorless [3]. The lightest neutralino $\tilde{\chi}_1^0$, which is a mixture of the superpartners of the neutral gauge and Higgs bosons, fulfills these conditions. In the following, it is assumed that R-parity is conserved and that $\tilde{\chi}_1^0$ is the LSP. Since this particle is weakly interacting, it escapes detection and provides the classic missing transverse energy ($\not\!\!E_T$) signature at colliders. In $p\bar{p}$ collisions, squarks ($\tilde{q}$) and gluinos ($\tilde{g}$), the superpartners of quarks and gluons, would be abundantly produced, if sufficiently light, by the strong interaction, leading to final states containing jets and $\not\!\!E_T$. The most constraining direct limits on squark and gluino masses were obtained by the D0 collaboration [4], based on an analysis of $310\,\mathrm{pb}^{-1}$ of data from $p\bar{p}$ collisions at a center-of-mass energy of 1.96 TeV, collected during Run II of the Fermilab Tevatron Collider. In the model of minimal supergravity (mSUGRA) [5], the limits obtained were $m_{\tilde{q}} > 325$ GeV and $m_{\tilde{g}} > 241$ GeV at the 95% C.L., for the set of model parameters detailed below. In this Letter, an update of the D0 search for squarks and gluinos in topologies with jets and large $\not\!\!E_T$ is reported, using a seven times larger data set of $2.1\,\mathrm{fb}^{-1}$.

A detailed description of the D0 detector can be found in Ref. [6]. The central tracking system consists of a silicon microstrip tracker and a central fiber tracker, both located within a 2 T superconducting solenoidal magnet. A liquid-argon and uranium calorimeter covers pseudorapidities up to $|\eta| \approx 4.2$, where $\eta = -\ln[\tan(\theta/2)]$, and θ is the polar angle with respect to the proton beam direction. The calorimeter consists of three sections, housed in separate cryostats: the central one covers $|\eta| \lesssim 1.1$, and the two end sections extend the coverage to larger $|\eta|$. The calorimeter is segmented in depth, with four electromagnetic layers followed by up to five hadronic layers. It is also segmented in semi-projective towers of size 0.1×0.1 in the (η, ϕ) plane, where ϕ is the azimuthal angle in radians. Calorimeter cells are defined by the intersections of towers and layers. Additional sampling is provided by scintillating tiles between cryostats. An outer muon system, covering $|\eta| < 2$, consists of a layer of tracking detectors and scintillation trigger counters in front of 1.8 T iron toroids, followed by two similar layers after the toroids. Jets were reconstructed with the iterative midpoint cone algorithm [7] with cone radius $\mathcal{R} = \sqrt{(\Delta\phi)^2 + (\Delta y)^2} = 0.5$ in azimuthal angle ϕ and rapidity $y = \frac{1}{2}\ln((E + p_z)/(E - p_z))$. The jet energy scale (JES) was derived from the transverse momentum balance in photon-plus-jet events. The $\not\!\!E_T$ was calculated from all calorimeter cells, and corrected for the jet energy scale and for the transverse momenta of reconstructed muons.

The D0 trigger system consists of three levels, L1, L2 and L3. The $1.2\,\mathrm{fb}^{-1}$ of data recorded after 2006 (during the so-called Run IIb) were collected using a significantly upgraded system, in particular a new L1 calorimeter trigger [8] involving a sliding-window algorithm which improved the jet triggering efficiency. In addition, $\not\!\!E_T$ was used at L1 to select events, which was not done during the previous data taking period (Run IIa). Both improvements helped to keep a high trigger efficiency despite the increased instantaneous luminosity in Run IIb (up to $2.8 \times 10^{32}\mathrm{cm}^{-2}\mathrm{s}^{-1}$, to be compared to $1.6 \times 10^{32}\mathrm{cm}^{-2}\mathrm{s}^{-1}$ in Run IIa). The events used in this analysis were recorded using two categories of triggers [9]. The dijet triggers selected events with two jets and $\not\!\!E_T$, while the multijet triggers were optimized for events with at least three jets and $\not\!\!E_T$.

The SM processes leading to events with jets and real $\not\!\!E_T$ in the final state ("SM backgrounds") are the production of W or Z bosons in association with jets (W/Z+jets), of pairs of vector bosons (WW, WZ, ZZ) or top quarks ($t\bar{t}$), and of single top quarks. The neutrinos from the decays $Z \to \nu\bar{\nu}$ and $W \to l\nu$, with the W boson produced directly or coming from a top quark decay, generate the $\not\!\!E_T$ signature. In this analysis, most of the W boson leptonic decays leading to an electron or a muon were identified, and the corresponding events rejected. However, a charged lepton from W boson decay can be a tau decaying hadronically. It can also be an electron or a muon that escapes detection or fails the identification criteria. Such W+jets events therefore exhibit the jets plus $\not\!\!E_T$ signature. Finally, multijet production also leads to a final state with jets and $\not\!\!E_T$ when one or more jets are mismeasured ("QCD background").

Events from SM and supersymmetric processes were simulated using Monte Carlo (MC) generators and passed through a full GEANT3-based [10] simulation of the detector geometry and response. They were subsequently processed with the same reconstruction chain as the data. The parton density functions (PDFs) used in the MC generators are the CTEQ6L1 [11] PDFs. A data event from a randomly selected beam crossing was overlaid on

each event to simulate the additional minimum bias interactions. The QCD background was not simulated, but estimated directly from data. The ALPGEN generator [12] was used to simulate $W/Z+$jets and $t\bar{t}$ production. It was interfaced with PYTHIA [13] for the simulation of initial and final state radiation (ISR/FSR) and of jet hadronization. Pairs of vector bosons and electroweak top quark production were simulated with PYTHIA and COMPHEP [14], respectively. The next-to-leading order (NLO) cross sections were computed with MCFM 5.1 [15].

Squark and gluino production and decay were simulated with PYTHIA. The masses of the supersymmetric particles were calculated with SUSPECT 2.3 [16] from the set of five mSUGRA parameters: m_0, the universal scalar mass at the grand unification scale $\Lambda_{\rm GUT}$; $m_{1/2}$ the universal gaugino mass at $\Lambda_{\rm GUT}$; A_0, the universal trilinear coupling at $\Lambda_{\rm GUT}$; $\tan\beta$, the ratio of the vacuum expectation values of the two Higgs fields; and μ the sign of the Higgs-mixing mass parameter. The decay widths and branching ratios of all supersymmetric particles were then calculated with SDECAY 1.1A [17]. In order to allow for an easier comparison with previous results, the following parameters were fixed to the same values as in Ref. [4]: $A_0 = 0$, $\tan\beta = 3$, and $\mu < 0$. The production of scalar top quarks (stops) was ignored, and in the following, the "squark mass" is the average mass of all squarks other than stops. All squark and gluino decay modes were taken into account, including cascade decays through charginos or neutralinos which could additionally produce electrons, muons, or taus. The NLO cross sections of the squark and gluino pair production were calculated with PROSPINO 2 [18].

The analysis strategy is the same as in Ref. [4] with three analyses optimized for three benchmark regions of the mSUGRA parameter space. A "dijet" analysis was optimized at low m_0 for events containing a pair of acoplanar jets, as expected from $p\bar{p} \to \tilde{q}\bar{\tilde{q}} \to q\tilde{\chi}_1^0\bar{q}\tilde{\chi}_1^0$ and $p\bar{p} \to \tilde{q}\tilde{q} \to q\tilde{\chi}_1^0 q\tilde{\chi}_1^0$. A "gluino" analysis was optimized at high m_0 for events with at least four jets, as expected from $p\bar{p} \to \tilde{g}\tilde{g} \to q\bar{q}\tilde{\chi}_1^0 q\bar{q}\tilde{\chi}_1^0$. Finally, a "3-jets" analysis was optimized for events with at least three jets, as expected from $p\bar{p} \to \tilde{q}\tilde{g} \to q\tilde{\chi}_1^0 q\bar{q}\tilde{\chi}_1^0$. The benchmark for this analysis is the case where $m_{\tilde{q}} = m_{\tilde{g}}$.

Each analysis required at least two jets and substantial $\not\!\!E_T$ (≥ 40 GeV). The acoplanarity, i.e. the azimuthal angle between the two leading jets, was required to be smaller than 165°, where the two leading jets are those with the largest transverse momenta. These leading jets were required: to be in the central region of the calorimeter, $|\eta_{\rm det}| < 0.8$, where $\eta_{\rm det}$ is the jet pseudorapidity calculated under the assumption that the jet originates from the detector center; to have fractions of energy in the electromagnetic layers of the calorimeter less than 0.95; and to have transverse momenta greater than 35 GeV. The best primary vertex (PV0) was selected among all reconstructed primary vertices (PV) as the one with the smallest probability to be due to a minimum bias interaction [19]. Its longitudinal position with respect to the detector center was restricted to $|z| < 60$ cm to ensure efficient reconstruction. For each jet, CPF0 is defined as the fraction of track p_T sum associated with the jet which comes from PV0, CPF0= $\sum p_T^{\rm track}({\rm PV0}) / \sum p_T^{\rm track}({\rm any\ PV})$. The two leading jets were required to have CPF0 larger than 0.75. Since jet transverse momenta and $\not\!\!E_T$ were calculated with respect to PV0, this criterion reduced the background with large $\not\!\!E_T$ due to an incorrect PV0 selection.

TABLE I: Selection criteria for the three analyses (all energies and momenta in GeV); see the text for further details.

Preselection Cut		All Analyses	
$\not\!\!E_T$		≥ 40	
|Vertex z pos.|		< 60 cm	
Acoplanarity		$< 165°$	
Selection Cut	"dijet"	"3-jets"	"gluino"
Trigger	dijet	multijet	multijet
jet$_1$ p_T [a]	≥ 35	≥ 35	≥ 35
jet$_2$ p_T [a]	≥ 35	≥ 35	≥ 35
jet$_3$ p_T [b]	–	≥ 35	≥ 35
jet$_4$ p_T [b]	–	–	≥ 20
Electron veto	yes	yes	yes
Muon veto	yes	yes	yes
$\Delta\phi(\not\!\!E_T, {\rm jet}_1)$	$\geq 90°$	$\geq 90°$	$\geq 90°$
$\Delta\phi(\not\!\!E_T, {\rm jet}_2)$	$\geq 50°$	$\geq 50°$	$\geq 50°$
$\Delta\phi_{\rm min}(\not\!\!E_T, {\rm any\ jet})$	$\geq 40°$	–	–
H_T	≥ 325	≥ 375	≥ 400
$\not\!\!E_T$	≥ 225	≥ 175	≥ 100

[a] First and second jets are also required to be central ($|\eta_{\rm det}| < 0.8$), with an electromagnetic fraction below 0.95, and to have CPF0 ≥ 0.75.

[b] Third and fourth jets are required to have $|\eta_{\rm det}| < 2.5$, with an electromagnetic fraction below 0.95.

Different selection criteria were applied in the three analyses, as summarized in Table I. Events passing a trigger for acoplanar dijet events were used in the "dijet" analysis, while a multijet and $\not\!\!E_T$ trigger was required in the "3-jets" and "gluino" analyses. In the "3-jets" and "gluino" analyses, a third and fourth jet were required, respectively. In comparison with the previously published analysis [4], the $|\eta_{\rm det}|$ upper limit for the third and fourth jet was increased from 0.8 to 2.5, which considerably improved the signal efficiency at high m_0. These two jets also had to have their fraction of energy in the electromagnetic layers of the calorimeter less than 0.95, but no requirement was made on their CPF0. The third and fourth jet transverse momenta were required to exceed 35 GeV and 20 GeV, respectively. In all three analyses, a veto on isolated electrons or muons with $p_T > 10$ GeV was applied to reject background events containing a leptonic W boson decay. The azimuthal angles between the $\not\!\!E_T$ and the first jet, $\Delta\phi(\not\!\!E_T, {\rm jet}_1)$, and the second jet, $\Delta\phi(\not\!\!E_T, {\rm jet}_2)$, were used to remove events where the en-

ergy of one jet was mismeasured, generating $\not\!\!E_T$ aligned with that jet. In the "dijet" analysis, the minimum azimuthal angle $\Delta\phi_{\rm min}(\not\!\!E_T, \text{any jet})$ between the $\not\!\!E_T$ and any jet with $p_T > 15\,\text{GeV}$ was required to be greater than 40° to further suppress QCD background. This criterion was not used in the "3-jets" and "gluino" analyses because of the higher jet multiplicity in the signal events.

The two final cuts on $\not\!\!E_T$ and on $H_T = \sum_{\rm jets} p_T$, where the sum is over all jets with $p_T > 15\,\text{GeV}$ and $|\eta_{\rm det}| < 2.5$, were optimized by minimizing the expected upper limit on the cross section in the absence of signal. Here and in the calculation of the final limits, the modified frequentist CL_s method [20] was used. The QCD background contribution was estimated by fitting the $\not\!\!E_T$ distribution below 60 GeV with an exponential function, after subtraction of the SM background processes, and subsequently extrapolating this function above the chosen $\not\!\!E_T$ cut value. The optimal cuts are given in Table I. The $\not\!\!E_T$ distributions after applying all analysis criteria except the one on $\not\!\!E_T$ are shown in Fig. 1 for the three analyses.

Table II reports the number of data events and the expected signal and background. The main background contributions are from $(Z \to \nu\bar{\nu}) + \text{jets}$, $(W \to l\nu) + \text{jets}$, and $t\bar{t} \to b\bar{b}\,q\bar{q}'l\nu$. The QCD background was evaluated from a fit to the $\not\!\!E_T$ distribution as described above. The largest QCD contribution of 1.4 ± 0.8 event was estimated in the "gluino" analysis, but was conservatively ignored when setting the limits. It was found to be negligible in the "dijet" and "3-jets" analyses. The signal efficiencies are given in Table II for the three benchmark scenarios, with the corresponding values of m_0, $m_{1/2}$, the squark and gluino masses, and the NLO cross section.

The uncertainty coming from the JES corrections is typically (10–15)% for the SM backgrounds and (6–11)% for the signal efficiencies. The uncertainties due to the jet energy resolution, to the jet track confirmation, and to jet reconstruction and identification efficiencies range between 2% and 4%. All these uncertainties on jet properties account for differences between data and MC simulation, both for signal efficiencies and background contributions. The trigger was found to be fully efficient for the event samples surviving all analysis cuts with an uncertainty of 2%. The uncertainty on the luminosity measurement is 6.1% [21]. All of these uncertainties are fully correlated between signal and SM backgrounds. A 15% systematic uncertainty was set on the W/Z+jets and $t\bar{t}$ NLO cross sections. The uncertainty on the signal acceptance due to the PDF choice was determined to be 6%, using the forty-eigenvector basis of the CTEQ6.1M PDF set [11]. Finally, the effects of ISR/FSR on the signal efficiencies were studied by varying the PYTHIA parameters controlling the QCD scales and the maximal allowed virtualities used in the simulation of the space-like and time-like parton showers. The uncertainty on the signal efficiencies was determined to be 6%.

The nominal NLO signal cross sections, $\sigma_{\rm nom}$, were computed with the CTEQ6.1M PDF and for the renormalization and factorization scale $\mu_{\rm r,f} = Q$, where Q was taken to be equal to $m_{\tilde{g}}$ for $\tilde{g}\tilde{g}$ production, $m_{\tilde{q}}$ for $\tilde{q}\tilde{q}$ and $\tilde{q}\bar{\tilde{q}}$ production, and $(m_{\tilde{q}} + m_{\tilde{g}})/2$ for $\tilde{q}\tilde{g}$ production. The uncertainty due to the choice of PDF was determined using the full set of CTEQ6.1M eigenvectors, with the individual uncertainties added in quadrature. The effect on the nominal signal cross sections, which varies between 15% and 60%, is dominated by the large uncertainty on the gluon distribution at high x. The effect of the renormalization and factorization scale was studied by calculating the signal cross sections for $\mu_{\rm r,f} = Q$, $\mu_{\rm r,f} = Q/2$ and $\mu_{\rm r,f} = 2 \times Q$. The factor of two on this scale reduces or increases the nominal signal cross sections by (15–20)%. The PDF and $\mu_{\rm r,f}$ effects were added in quadrature to compute minimum, $\sigma_{\rm min}$, and maximum, $\sigma_{\rm max}$, signal cross sections.

The numbers of events observed in the data are in agreement with the SM background expectation in the three analyses. Therefore, an excluded domain in the gluino-squark mass plane was determined as follows. The three analyses were run over signal MC samples generated in the gluino-squark mass plane to compute signal efficiencies. Then, to take advantage of the different features of the three analyses, seven independent combinations of the three selections were defined as shown in Table III, which were combined in the limit computations. The number of events passing at least one of the three analyses is 31 while the SM expectation is $32.6 \pm 1.7(\text{stat.})^{+9.0}_{-5.8}(\text{syst.})$ events. Figure 2 shows the 95% C.L. observed and expected upper limits on squark-gluino production cross sections for the three benchmark scenarios. Figure 3 shows the excluded domain in the gluino-squark mass plane.

The absolute lower limits on the squark and gluino masses obtained in the most conservative hypothesis, $\sigma_{\rm min}$, are 379 GeV and 308 GeV, respectively. The corresponding expected limits are 377 GeV and 312 GeV. Table IV summarizes these absolute limits for the three signal cross section hypotheses. Limits were also derived for the particular case $m_{\tilde{q}} = m_{\tilde{g}}$. For $\sigma_{\rm min}$, squark and gluino masses below 390 GeV are excluded, while the expected limit is 390 GeV. The observed limit becomes 408 GeV for $\sigma_{\rm nom}$, and 427 GeV for $\sigma_{\rm max}$.

The results of this analysis also constrain the mSUGRA parameters at the grand unification scale. Figure 4 shows the excluded regions in the $(m_0, m_{1/2})$ plane for $\tan\beta = 3$, $A_0 = 0$, $\mu < 0$. Although a detailed scan of the mSUGRA parameter space is beyond the scope of this analysis, it was verified that similar results hold for a large class of parameter sets. In particular, the fact that there is no explicit veto in this analysis on hadronically decaying tau leptons mitigates the expected efficiency reduction at larger values of $\tan\beta$. It can be seen in Fig. 4 that the limits from LEP2 chargino and slepton searches [23] are improved for m_0 values between 70 and

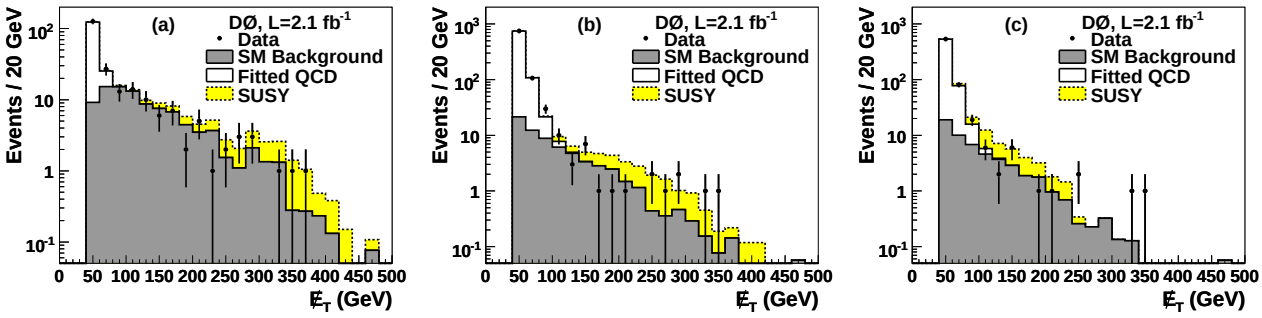

FIG. 1: Distributions of $\not\!\!E_T$ after applying all analysis criteria except the one on $\not\!\!E_T$ for the "dijet" (a), "3-jets" (b), and "gluino" (c) analyses; for data (points with error bars), for SM background (full histogram), and for signal MC (dotted histogram on top of SM). The signal drawn corresponds to $(m_0, m_{1/2}) = (25, 175)$ GeV, $m_{\tilde{q}} = m_{\tilde{g}} = 410$ GeV, and $(m_0, m_{1/2}) = (500, 110)$ GeV from left to right. The fitted QCD background contribution is also shown.

TABLE II: For each analysis, information on the signal for which it was optimized (m_0, $m_{1/2}$, $m_{\tilde{g}}$, $m_{\tilde{q}}$, and nominal NLO cross section), signal efficiency, the number of events observed, the number of events expected from SM backgrounds, the number of events expected from signal, and the 95% C.L. signal cross section upper limit. The first uncertainty is statistical and the second is systematic.

Analysis	$(m_0, m_{1/2})$ (GeV)	$(m_{\tilde{g}}, m_{\tilde{q}})$ (GeV)	$\sigma_{\rm nom}$ (pb)	$\epsilon_{\rm sig.}$ (%)	$N_{\rm obs.}$	$N_{\rm backgrd.}$	$N_{\rm sig.}$	σ_{95} (pb)
"dijet"	(25,175)	(439,396)	0.072	$6.8 \pm 0.4^{+1.2}_{-1.2}$	11	$11.1 \pm 1.2^{+2.9}_{-2.3}$	$10.4 \pm 0.6^{+1.8}_{-1.8}$	0.075
"3-jets"	(197,154)	(400,400)	0.083	$6.8 \pm 0.4^{+1.4}_{-1.3}$	9	$10.7 \pm 0.9^{+3.1}_{-2.1}$	$12.0 \pm 0.7^{+2.5}_{-2.3}$	0.065
"gluino"	(500,110)	(320,551)	0.195	$4.1 \pm 0.3^{+0.8}_{-0.7}$	20	$17.7 \pm 1.1^{+5.5}_{-3.3}$	$17.0 \pm 1.2^{+3.3}_{-2.9}$	0.165

TABLE III: Definition of the analysis combinations, and number of events observed in the data and expected from the SM backgrounds.

Selection	"dijet"	"3-jets"	"gluino"	$N_{\rm obs.}$	$N_{\rm backgrd.}$
Combination 1	yes	no	no	8	9.4 ± 1.2 (stat.) $^{+2.3}_{-1.8}$ (syst.)
Combination 2	no	yes	no	2	4.5 ± 0.6 (stat.) $^{+0.7}_{-0.5}$ (syst.)
Combination 3	no	no	yes	14	12.5 ± 0.9 (stat.) $^{+3.6}_{-1.9}$ (syst.)
Combination 4	yes	yes	no	1	1.1 ± 0.3 (stat.) $^{+0.5}_{-0.3}$ (syst.)
Combination 5	yes	no	yes		kinematically not allowed
Combination 6	no	yes	yes	4	4.5 ± 0.6 (stat.) $^{+1.8}_{-1.3}$ (syst.)
Combination 7	yes	yes	yes	2	0.6 ± 0.2 (stat.) $^{+0.1}_{-0.2}$ (syst.)
At least one selection				31	32.6 ± 1.7 (stat.) $^{+9.0}_{-5.8}$ (syst.)

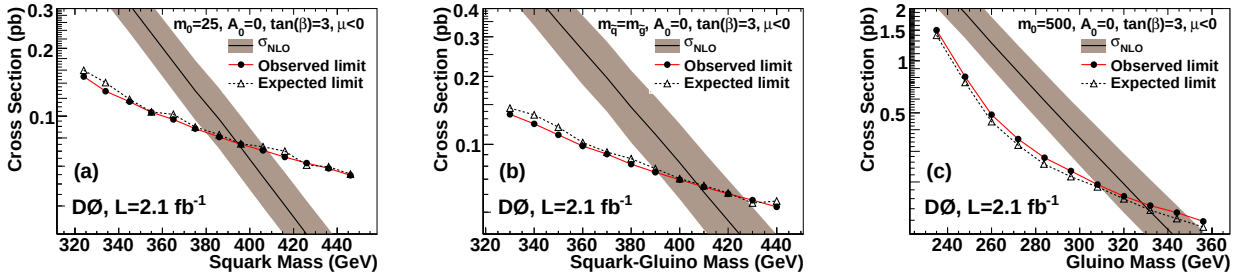

FIG. 2: For $\tan\beta = 3$, $A_0 = 0$, $\mu < 0$, observed (closed circles) and expected (opened triangles) 95% C.L. upper limits on squark-gluino production cross sections combining the analyses for $m_0 = 25$ GeV (a), $m_{\tilde{q}} = m_{\tilde{g}}$ (b), and $m_0 = 500$ GeV (c). The nominal production cross sections are also shown, with shaded bands corresponding to the PDF and renormalization-and-factorization scale uncertainties.

TABLE IV: Absolute lower limits at the 95% C.L. on the squark and gluino masses (in GeV) as a function of the choice of signal cross section hypothesis as defined in the text. Numbers in parentheses correspond to the expected limits. These limits are valid for the mSUGRA parameters $\tan\beta = 3$, $A_0 = 0$, $\mu < 0$.

Hypothesis	Gluino mass	Squark mass
$\sigma_{\rm min}$	308 (312)	379 (377)
$\sigma_{\rm nom}$	327 (332)	392 (391)
$\sigma_{\rm max}$	349 (354)	406 (404)

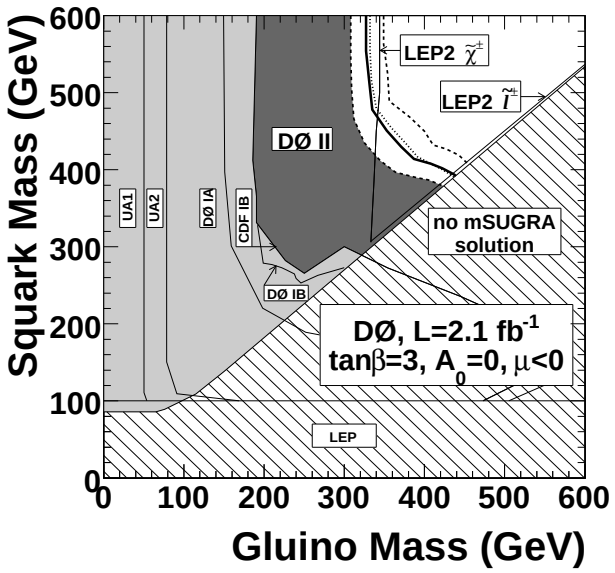

FIG. 3: In the gluino and squark mass plane, excluded regions at the 95% C.L. by direct searches in the mSUGRA framework with $\tan\beta = 3$, $A_0 = 0$, $\mu < 0$. The region excluded by this analysis and previous D0 Run II results [4] in the most conservative hypothesis ($\sigma_{\rm min}$) is shown in dark shading. The thick (dotted) line is the limit of the observed (expected) excluded region for the $\sigma_{\rm nom}$ hypothesis. The band delimited by the two dashed lines shows the effect of the PDF choice and of the variation of $\mu_{\rm r,f}$ by a factor of two. Regions excluded by previous experiments are indicated in light shading [22]. The two thin lines indicate the indirect limits inferred from the LEP2 chargino and slepton searches [23]. The region where no mSUGRA solution can be found is shown hatched.

300 GeV and for $m_{1/2}$ values between 125 and 165 GeV. However, the LEP2 Higgs search limits remain more constraining in a purely mSUGRA scenario [23].

In summary, a search for squarks and gluinos produced in $p\bar{p}$ collisions at 1.96 TeV has been performed in a 2.1 fb^{-1} data sample. The results of three selections of events with jets and large missing transverse energy are in agreement with the SM background predictions. In the framework of minimal supergravity with $\tan\beta = 3$,

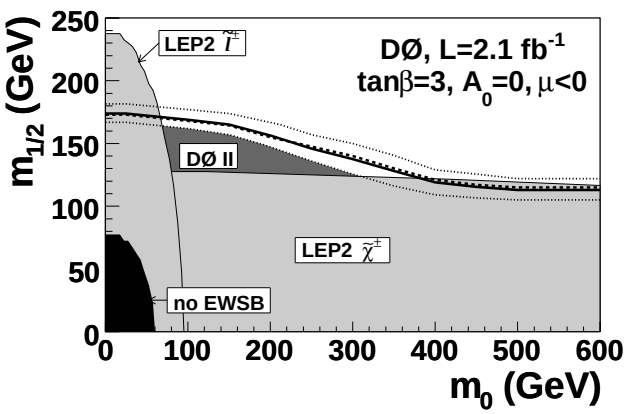

FIG. 4: In the $(m_0, m_{1/2})$ plane, the region excluded by this analysis at the 95% C.L. in the mSUGRA framework for $\tan\beta = 3$, $A_0 = 0$, $\mu < 0$ is shown in dark shading. The thick line is the limit of the excluded region for the $\sigma_{\rm nom}$ hypothesis. The corresponding expected limit is the dashed line. The band delimited by the two dotted lines shows the effect of the PDF choice and of the variation of $\mu_{\rm r,f}$ by a factor of two. Regions excluded by the LEP2 chargino and slepton searches are indicated in light shading [23]. The region where there is no electroweak symmetry breaking is shown in black.

$A_0 = 0$, and $\mu < 0$, 95% C.L. lower limits of 392 GeV and 327 GeV were set on the squark and gluino masses, respectively, for the central choice of PDF and for a renormalization and factorization scale equal to the mass of the squark or gluino produced. Taking into account the PDF uncertainties and allowing for a factor of two in the choice of scale, these limits are reduced to 379 GeV and 308 GeV. They exceed the corresponding previous limits [4] by 54 GeV and 67 GeV and are the most constraining direct limits on the squark and gluino masses to date.

We thank the staffs at Fermilab and collaborating institutions, and acknowledge support from the DOE and NSF (USA); CEA and CNRS/IN2P3 (France); FASI, Rosatom and RFBR (Russia); CAPES, CNPq, FAPERJ, FAPESP and FUNDUNESP (Brazil); DAE and DST (India); Colciencias (Colombia); CONACyT (Mexico); KRF and KOSEF (Korea); CONICET and UBACyT (Argentina); FOM (The Netherlands); Science and Technology Facilities Council (United Kingdom); MSMT and GACR (Czech Republic); CRC Program, CFI, NSERC and WestGrid Project (Canada); BMBF and DFG (Germany); SFI (Ireland); The Swedish Research Council (Sweden); CAS and CNSF (China); and the Alexander von Humboldt Foundation.

[a] Visitor from Augustana College, Sioux Falls, SD, USA.
[b] Visitor from The University of Liverpool, Liverpool, UK.

[c] Visitor from ICN-UNAM, Mexico City, Mexico.
[d] Visitor from II. Physikalisches Institut, Georg-August-University, Göttingen, Germany.
[e] Visitor from Helsinki Institute of Physics, Helsinki, Finland.
[†] Fermilab International Fellow.
[‡] Deceased.

[1] H.E. Haber and G.L. Kane, Phys. Rep. **117**, 75 (1985).
[2] P. Fayet, Phys. Lett. B **69**, 489 (1977).
[3] J. Ellis *et al.*, Nucl. Phys. **B238**, 453 (1984).
[4] V.M. Abazov *et al.* (D0 Collaboration), Phys. Lett. B **638**, 119 (2006).
[5] H.P. Nilles, Phys. Rep. **110**, 1 (1984).
[6] V.M. Abazov *et al.* (D0 Collaboration), Nucl. Instrum. Methods in Phys. Res. A **565**, 463 (2006).
[7] G.C. Blazey *et al.*, in *Proceedings of the Workhop: "QCD and Weak Boson Physics in Run II,"* edited by U. Baur, R.K. Ellis, and D. Zeppenfeld (Fermilab, Batavia, IL, 2000), p. 47; see Sec. 3.5 for details.
[8] M. Abolins *et al.*, Nucl. Instrum. Methods in Phys. Res. A **584/1**, 75 (2007).
[9] T. Millet, PhD Thesis, unpublished, FERMILAB-THESIS-2007-22, LYCEN-T-2007-09.
[10] R. Brun and F. Carminati, CERN Program Library Long Writeup W5013, 1993 (unpublished).
[11] J. Pumplin *et al.*, JHEP **0207**, 012 (2002); D. Stump *et al.*, JHEP **0310**, 046 (2003).
[12] M.L. Mangano *et al.*, JHEP **0307**, 001 (2003); version 2.05 (2.11) was used for Run IIa (Run IIb) simulation.
[13] T. Sjöstrand, S. Mrenna and P. Skands, JHEP **0605**, 026 (2006); version 6.323 (6.409) was used for Run IIa (Run IIb) simulation.
[14] E. Boos *et al.* (CompHEP Collaboration), Nucl. Instrum. Methods in Phys. Res. A **534**, 250 (2004).
[15] J.M. Campbell and R.K. Ellis, Phys. Rev. D **60**, 113006 (1999).
[16] A. Djouadi, J.L. Kneur and G. Moultaka, Comput. Phys. Commun. **176**, 426 (2007).
[17] M. Muhlleitner, A. Djouadi and Y. Mambrini, Comput. Phys. Commun. **168**, 46 (2005).
[18] W. Beenakker, R. Hopker, M. Spira and P.M. Zerwas, Nucl. Phys. **B492**, 51 (1997).
[19] V.M. Abazov *et al.* (D0 Collaboration), Phys. Rev. D **74**, 112004 (2006).
[20] T. Junk, Nucl. Instrum. Methods in Phys. Res. A **434**, 435 (1999); A. Read, in *"1st Workshop on Confidence Limits,"* CERN Report No. CERN-2000-005, 2000.
[21] T. Andeen *et al.*, FERMILAB-TM-2365 (2007).
[22] C. Albajar *et al.* (UA1 Collaboration), Phys. Lett. B **198**, 261 (1987); J. Alitti *et al.* (UA2 Collaboration), Phys. Lett. B **235**, 363 (1990); S. Abachi *et al.* (D0 Collaboration), Phys. Rev. Lett. **75**, 618 (1995); B. Abbott *et al.* (D0 Collaboration), Phys. Rev. Lett. **83**, 4937 (1999); T. Affolder *et al.* (CDF Collaboration), Phys. Rev. Lett. **88**, 041801 (2002); A. Heister *et al.* (ALEPH Collaboration), Phys. Lett. B **537**, 5 (2002); P. Achard *et al.* (L3 Collaboration), Phys. Lett. B **580**, 37 (2004).
[23] LEPSUSYWG, ALEPH, DELPHI, L3 and OPAL collaborations, note LEPSUSYWG/02-06.2 (http://lepsusy.web.cern.ch/lepsusy/).